DYNAMIC STRUCTURES IN OCEAN WATERS AND SUSPENSION MICROPHYSICAL CHARACTERISTICS FROM HYDROOPTICAL MEASUREMENTS

A.A. Kumeisha, A.P. Ivanov, S.L. Oshchepkov, O.V. Dubovik, T.V. Lapenok, V.D. Kozlov, and N.A. Kumeisha

Institute of Physics,
Academy of Sciences of Belorus', Mogilev
Received May 17, 1994

The potentials of the hydrooptical measurements to determine the dynamic structures on different scales in ocean are discussed. The inversion method to obtain the size distribution of organic and mineral particles from volume scattering phase functions measurements in angular range from 1 *to* 170° *at* $\lambda = 525$ nm *as well as the results of processing* in situ *data obtained for Belorus' lakes are described.*

The process of compiling knowledge about geophysical characteristics of ocean and in–land waters as well as of biological parameters of water boicenoses is extremely long and too laborious. Limited possibilities of standard hydrological and biological methods provide only slow progress here. At the same time, some non–traditional optical methods of water monitoring which are capable not only to speed up the process of acquiring information but also to extend it.

As known, optical properties of water strongly depend on variations in the composition of water suspension which, in its turn, is very sensitive to any changes of external hydrophysical conditions. Thus, the optical properties can serve as indicators of hydrodynamic structures of different scales: from macrocirculation oceanic systems to small vortex formations frequently occurring in frontal zones.

Figure 1 illustrates the possibility of a more accurate determination of the boundaries of adjacent water masses in the ocean and the streams dividing them from the behavior of the extinction coefficient $\varepsilon(H)$. The studies were carried out in 1982–1986 in the Pacific Ocean on the quasi–meridian cross section along 160°E between 52° and 36°N. The structure of temperature field is shown in Fig. 1 *a*. In accordance with this structure, zone I corresponds to the area occupied by subpolar waters; zone IV corresponds to subtropical, and zones II and III correspond to the North–Pacific stream with double–frontal structure[1] dividing them. The extinction coefficient profiles typical for these zones as well as vertical distributions of temperature and salinity are shown schematically in Figs. 1 *b–e*. As one can see, the change from subpolar (zone I) to subtropical (IV) waters goes through two sufficiently stable intermediate optical gradations (Figs. 1 *c* and *d*) characteristic of distinct zones II and III (Fig. 1 *a*) of subpolar front. The biological suspension descends together with cold subpolar water in zone II, forming maxima at 10–20 m propped up from below, as in zone I, by seasonal thermal ridge (albeit more diffuse). The cold water descends lower in zone III; the suspension maxima descend down to 60–75 m being lower than the thermal ridge. It is interesting that suspension maxima occur at the depths close to the levels of salinity extrema and "follow" them (Fig. 1 *a*). Thus, the analysis only of vertical structure of the transmission allows distinguishing between water from different masses or identification of characteristic parts of frontal zone (stream) and besides estimating the depths of maximum gradients of hydrological characteristics.

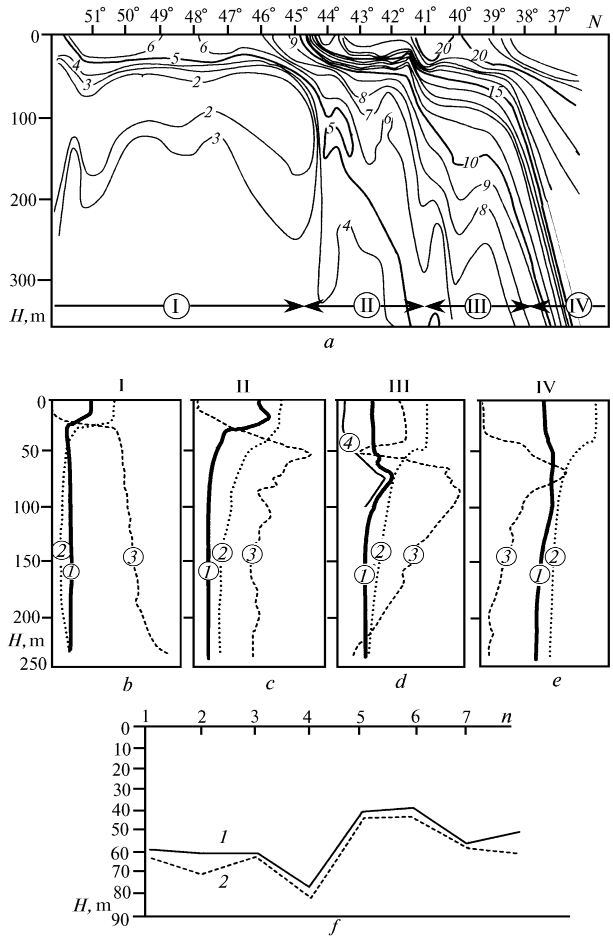

FIG. 1. Results of studies of subpolar front in the North–Western part of the Pacific Ocean: a map of temperature isolines (a); typical distributions of extinction coefficient (1), temperature (2), and salinity (3) sections (b–e); depths of levels of maxima of the extinction coefficient (1) and salinity (2) at the stations in zone III (f).

0235-6880/94/11–12 844-06 $02.00

Angular dependence of light scattering measured with a laboratory meter or scattering phase function[2] of surface water samples were used in the other example of oceanic waters identification. The work was done in vast area of the Greenlandian and Norwegian seas. As is shown in Fig. 2, where isolines of salinity are shown together with water temperature at the corresponding stations, a warm Western–Spitsbergian (center of the figure) and cold Greenlandian and Medvezhinskoe streams (left– and right–hand peripheries) are clearly seen in the area under study. It is natural to expect that waters of different origin have their own stable biocenoses and specific features in the scattering phase functions. The ratio of coefficients of directional scattering at small (3°) and large (45°) angles, characterizing properly the ratio of concentrations of coarse and fine fractions of suspension was chosen as an indicator of specific features in the scattering phase functions. As the analysis showed, more warm and salt waters of Western–Spitsbergian stream have high values of this parameter ($2{\cdot}10^3$–$3.3{\cdot}10^3$; solid circles denote the stations), while on cold waters streams it is low ($0.63{\cdot}10^3$–$1.1{\cdot}10^3$; open circles). The intermediate values (gray shading) are characteristic of waters in boundary areas. Thus, optical information is quite useful for studying water mass dynamics in more detail.

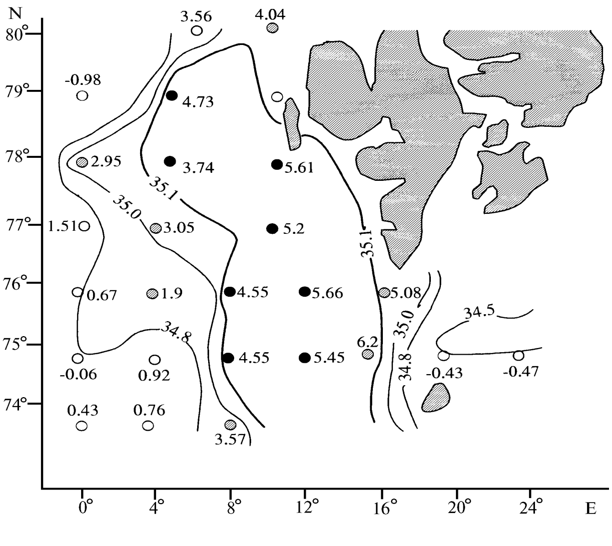

FIG. 2. Results of studies of water mass dynamics in the Greenlandian and Norwegian seas.

Let us come to discussion of the possibilities of making diagnostics of smaller synoptic dynamic structures. Local deviations of optical properties of a medium from the background ones (natural for the given water area) can be indicative of the presence of local anomalies in external hydrophysical conditions. For example, the more intense evolution of biological suspension in comparison with the background areas can be observed in zones of synoptic cyclonic vortexes, where the rise of depth waters rich of biogenous elements occur. This evolution manifests itself via enhanced values of scattering (extinction) characteristics and specific shape of transmission profiles. The relative oppression of phytoplankton evolution with corresponding changing of water optical properties occurs in zones of anticyclonic vortexes with inherently descending water motions.

In our paper,[3] the presence and the type of synoptic vortexes were diagnosed by peculiarities in vertical profiles of the extinction coefficient $\varepsilon(H)$ at the wavelength of 530 nm. Owing to demonstrated possibility of small–parameter representation of the profiles (using technique of empirical orthogonal components), we succeeded in characterizing their basic features (peculiarities) by a single parameter: the first coefficient of the expansion over eigenvectors of the covariation matrix with its numerical values being used as an indicator of water type. The map of isolines of the first coefficient is presented in Fig. 3 *a*; distribution of its value over stations is shown in Fig. 3 *b*. The classification of transmission profiles with respect to the value of the first expansion coefficient for a vast region of the Pacific ocean allowed the clear identification of vortex structures of cyclonic and anticyclonic types usually arising at the watershed boundary of two streams (a map of dynamic heights based on the results of hydrological survey is given in Fig. 3 *c* for a comparison) to be done.

The optical methods are also rather effective in a number of cases concerning diagnostics of near bottom streams which do not differ by hydrological characteristics from the above–lying waters but have different water transmission because of mixing sediments. Just this situation was observed during the mission to the Norwegian Sea where sharp bottom nepheloid layers were discovered (Fig. 4). The following optical studies in the same area were done by beam sections crossed at one point allowed also the determination of the direction of bottom stream to be done more accurately.

Let us now consider the possibilities of determining suspension microphysical characteristics from the data of optical measurements. It is known that optical properties of water characterising quantitatively the processes of light absorption and scattering by components of the water ecosystems, accumulate practically all information about these components. Thus, solving the inverse problem, it is possible to evaluate the concentration of organic matter and the content of submicron mineral particles, size–distribution function of suspension, concentration of chlorophyll and other pigments, and concentration of dissolved organic substance from optical data. Here we consider only the problem on determining particle size spectrum from data of measurements of angular dependences of scattering coefficient $\sigma(\gamma)$ at a single wavelength. The examples given below are connected with the processing of experimental data obtained in the water of typical Belorussian lakes, however the developed methods can also be used for interpretation of oceanic measurements.

It is assumed in our approach that natural hydrosol can be considered in general as a two–component system containing organic (phytoplankton + detrit) and mineral spherical particles which differ by both size r and complex index of refraction m ($r_{\text{org}} \geq 0.5\ \mu\text{m}$, $m_{\text{org}} = 1.05 - 0.0004\,i$ and $r_{\min} \leq 1\ \mu\text{m}$, $m_{\min} = 1.15 - 0.0001\,i$).

It is known, that $\sigma(\gamma)$ can be expressed as a sum of integrals:

$$\sigma(\gamma) = \sum_{n=1}^{2} \sigma'_n\,(\kappa\,r,\ m_n,\ \gamma)\,\frac{4}{3}\,\frac{V_n(r)}{\pi\,r^3}\,\mathrm{d}\,r, \qquad (1)$$

where $\kappa = 2\pi/\lambda$; λ is the wavelength in a dispersion medium; $V_n(r)$ are functions of volume–distribution of organic ($n = 1$) and mineral ($n = 2$) particles; $\sigma'_n(\kappa r,\ m_n,\ \gamma)$ is a differential scattering cross–section of a single particle of the nth component; γ is the scattering angle. Value $\sigma'(\kappa r,\ m_n,\ \gamma)$ may be calculated by Mie formulas.

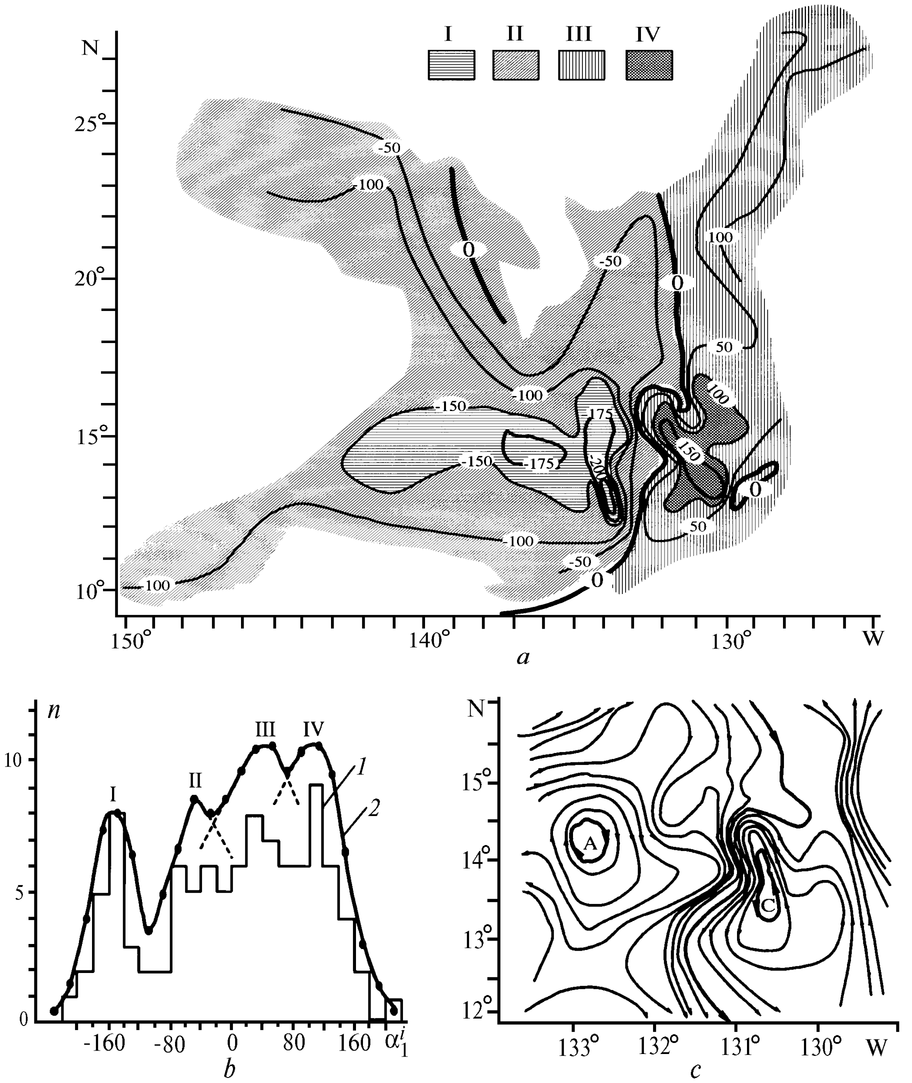

FIG. 3. Results of studies of synoptic vortex structures in the central part of tropical zone of the Pacific Ocean: the map of isolines of the first expansion coefficient α_1 *(a); the distribution of the number n of stations over the value of the first coefficient of expansion* α_1 *(histogram (1) and curve smoothed with the sliding window involving three steps (2)) (b). Roman figures I–IV denote groups of stations (waters) separated with respect to the value of the first expansion coefficient; and, the map of dynamic heights at the* 50–m *level based on the data of hydrological survey in the central part of the area under study (c).*

In numerical solution the formula (1) reduces to linear algebraic system by means of piecewise linear approximation of unknown $V_n(r)$. The obtained linear system may be inverted by the original method developed and described in Ref. 4. This procedure for single wavelength $\sigma(\gamma)$ is as follows

$$\begin{pmatrix}\mathbf{a}_1\\ \hline \mathbf{a}_2\end{pmatrix}^{q+1} = \begin{pmatrix}\mathbf{a}_1\\ \hline \mathbf{a}_2\end{pmatrix}^{q} - H^{q}\left[\left(U_1^q \,\middle|\, U_2^q\right)^{\mathrm{T}} (\mathbf{f}^{q} - \mathbf{f}^{*}) + \left(\begin{array}{c|c} g_1\,\Omega_{p_1} & 0\\ \hline 0 & g_2\,\Omega_{p_2}\end{array}\right)\begin{pmatrix}\mathbf{a}_1\\ \hline \mathbf{a}_2\end{pmatrix}^{q}\right], \qquad (2)$$

where superscript T denotes transposed matrix; diagonal matrix H^q consists of the elements

$$H_{i\,i}^{q} = \left\{\sum_{k=1}^{p_1+p_2}\left|\left\{\left(U_1^q \,\middle|\, U_2^q\right)^{\mathrm{T}}\left(U_1^q \,\middle|\, U_2^q\right) + \left(\begin{array}{c|c} g_1\,\Omega_{p_1} & 0\\ \hline 0 & g_2\,\Omega_{p_2}\end{array}\right)\right\}_{ik}\right|\right\}^{-1}; \qquad (3)$$

and matrix U_n^q consists of the elements $\{U_n^q\}_{j\,i_n} = \dfrac{\partial \ln\sigma_j}{\partial a_i}\Bigg|\begin{pmatrix}\mathbf{a}_1\\ \hline \mathbf{a}_2\end{pmatrix}^{q}$.

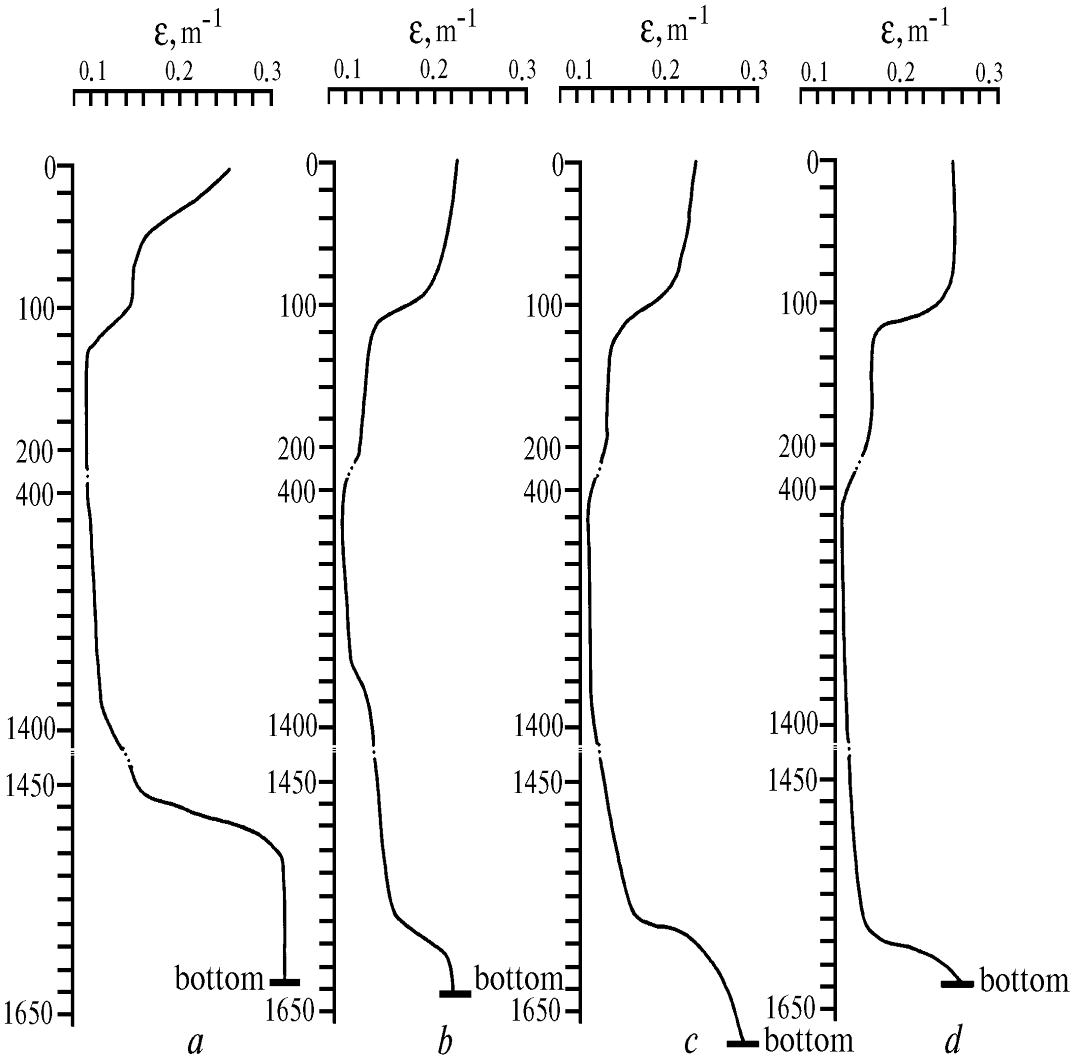

FIG. 4. Vertical structure of the extinction coefficient ε(H) at the four stations of latitudinal sections in the Norwegian sea. The separation between points a–d is approximately 7 miles.

In these relations **f*** and **a** are vector–columns of logarithms of measured, $\sigma(\gamma)$, and unknown, $V_n(r)$, values; subscripts j, i denote numbers of discrete angles of scattering and approximation $V_n(r)$ for organic ($i_1 = 1, 2, \ldots, p_1$) and mineral ($i_2 = 1, 2, \ldots, p_2$) particles; q is the number of iteration; Ω_{p_n} is a smoothing matrix used to limit variations of the second derivatives of a size spectrum of the nth component. The regularization parameters g_n were fitted in numerical experiments.

A special model experiment was carried out for checking the reliability of data obtained by the method developed for $\sigma(\gamma)$ inversion. It consisted in measuring the angular dependences of light scattering of the initial water sample from lake and three filtrates (extracted by filtering the initial sample through filters with pore sizes of 3, 1.5, and 0.41 μm) with the following reconstruction of particle size spectrum. The obtained results (volume concentrations of corresponding size groups) are presented in Fig. 5.

As is seen from the figure, if the total volume of large particles in the initial sample was about 2.4 ml/m^3, then the particles larger than 3 μm were not already observed after the first filter (the effect of "cutoff" is clearly seen in the figure), as a result the volume content of coarse fraction was reduced more than twice; after the second filter it is also halved, and the third filter detained practically the whole coarse fraction. As to the fine suspension, a small change in its concentration due to filtration is connected with the natural "blocking" of filter pores.

The developed mathematical algorithms were used for reconstruction of particle size spectra in the waters of typical Belorussian lakes by mass measurements during spring–summer period. The mean (normalized to the total volumes of corresponding fractions) particle size distribution functions were constructed from the obtained data (Fig. 6). As is seen, natural variability (indicated by standard deviations) is not large; the modal radius of organic particles was about 2 μm, that was confirmed by direct microscopic measurements.

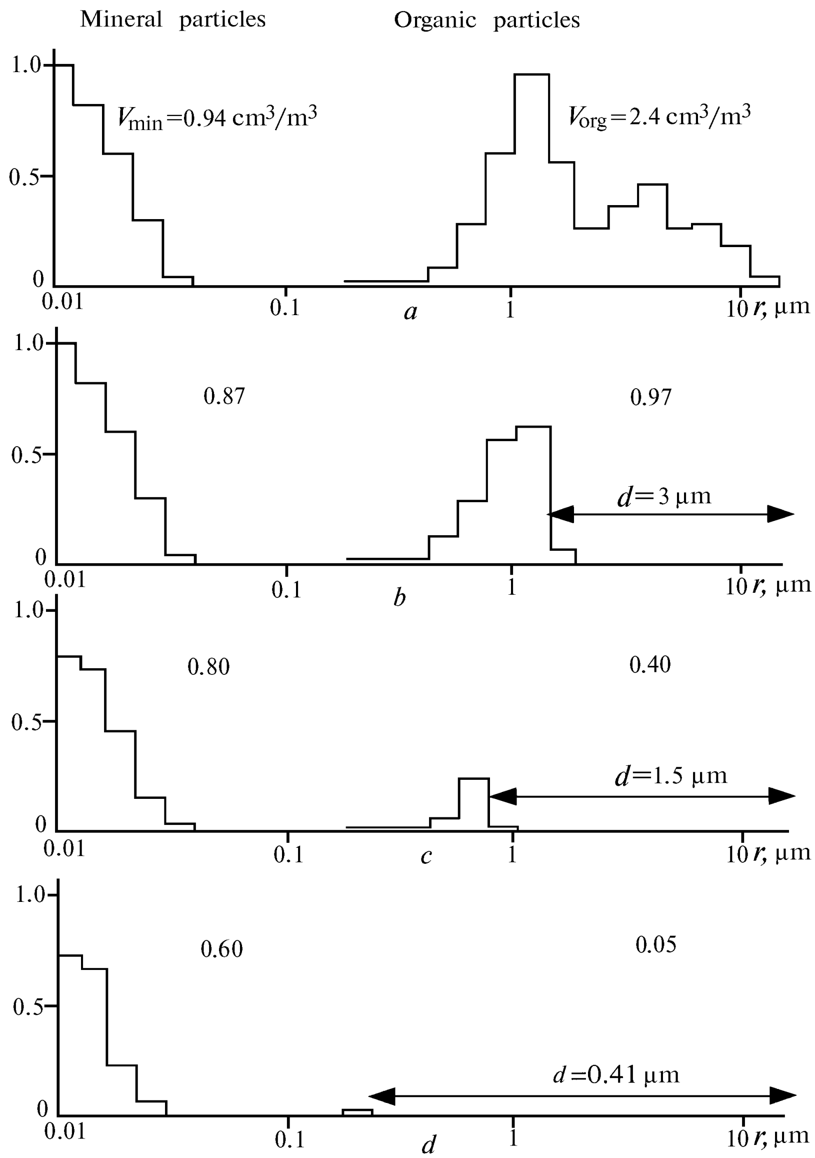

FIG. 5. Reconstructed distribution functions of volume concentrations of organic and mineral particles for initial sample of lake water (a) and three filtrates (b–d).

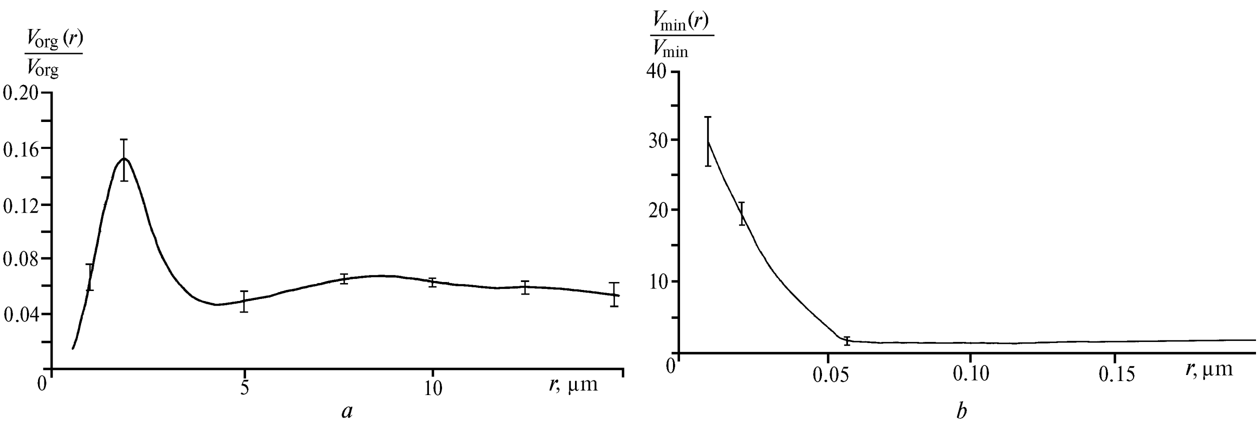

FIG. 6. Particle size distribution functions typical for open waters of Belorussian lakes (normalized to the total volume concentrations of corresponding fractions) in spring–summer period.

ACKNOWLEDGMENTS

In conclusion the authors would like to thank V.M.Fortus, G.Yu.Kosolapkin, and M.M.Korol' for help in conducting experimental measurements.

The authors A.A. Kumeisha and A.P. Ivanov acknowledge the International Scientific Foundation for partial support of this research.

REFERENCES

1. K.V. Moroshkin and K.D. Sabinin, Okeanologiya **24**, No. 3, 421–426 (1984).

2. A.V. Gavrilovich and A.P. Ivanov, "*Installation for a complex investigation into optical characteristics of light–scattering media,*" Preprint No. 470, Institute of Physics of the Academy of Sciences of the Belorussian SSR, Minsk (1975), 19 pp.

3. A.A. Kumeisha, Okeanologiya **32**, No. 1, 22–27 (1992).

4. O.V. Dubovik, S.L. Oshchepkov, and T.V. Lapenok, Izv. Ros. Akad. Nauk, Fiz. Atmos. Okeana **30**, No. 1, 106–113 (1994).